PFMAGO, a MAGO NASHI-Like Factor, Interacts with the MADS-Domain Protein MPF2 from *Physalis floridana*

Chaoying He, Hans Sommer, Britta Grosardt, Peter Huijser, and Heinz Saedler

Department of Molecular Plant Genetics, Max-Planck-Institute for Plant Breeding Research, Cologne, Germany

MADS-domain proteins serve as regulators of plant development and often form dimers and higher order complexes to function. Heterotopic expression of *MPF2*, a MADS-box gene, in reproductive tissues is a key component in the evolution of the inflated calyx syndrome in Physalis, but RNAi studies demonstrate that *MPF2* has also acquired a role in male fertility in *Physalis floridana*. Using the yeast 2-hybrid system, we have now identified numerous MPF2-interacting MADS-domain proteins from *Physalis*, including homologs of SOC1, AP1, SEP1, SEP3, AG, and AGL6. Among the many non-MADS-domain proteins recovered was a homolog of MAGO NASHI, a highly conserved RNA-binding protein known to be involved in many developmental processes including germ cell differentiation. Two MAGO genes, termed *P. floridana mago nashi1* (*PFMAGO1*) and *PFMAGO2*, were isolated from *P. floridana*. Both copies were found to be coexpressed in leaves, fruits, and, albeit at lower level, also in roots, stems, and flowers. DNA sequence analysis revealed that, although the coding sequences of the 2 genes are highly conserved, they differ substantially in their intron and promoter sequences. Two-hybrid screening of a *Physalis* expression library with both PFMAGO1 and PFMAGO2 as baits yielded numerous gene products, including an Y14-like protein. Y14 is an RNA-binding protein that forms part of various "gene expression machines." The function of MPF2 and 2 PFMAGO proteins in ensuring male fertility and evolution of calyx development in *Physalis* is discussed.

Introduction

Inflated Calyx Syndrome (ICS), otherwise known as the Chinese lantern, is a morphological novelty that has evolved multiple times in the plant family Solanaceae (He et al. 2004; He and Saedler 2005). In species that display ICS, such as *Physalis floridana*, the calyx (which is derived from the first floral whorl) undergoes a striking change in architecture during flower and fruit development, ultimately forming a balloon-like structure that encloses the mature berry. No such changes occur in the architecture of first-whorl organs in many other solanaceous species, for example, *Solanum tuberosum*, in which the calyx remains small throughout development. Recruitment of MPF2, a MADS-domain protein otherwise expressed only in vegetative tissues, into a floral context in a progenitor of *Physalis*, apparently led to the evolution of this novel trait, which is characteristic of this genus. Sequence changes in the promoter are believed to be responsible for the heterotopic expression of *MPF2* that leads to the ICS in *P. floridana* (He and Saedler 2005). Furthermore, RNAi experiments have revealed that *MPF2* is also essential for normal male fertility in *P. floridana* (He and Saedler 2005).

Plant MADS-domain proteins (Sommer et al. 1990; Yanofsky et al. 1990) often play key roles in diverse aspects of development and organogenesis (Theissen 2001). These DNA-binding proteins can act either as repressors or activators in the regulation of developmental processes. Usually they are believed to function as dimers or even as oligomers. Only in a few instances are MADS-domain proteins known to act as homodimers (Masiero et al. 2004; Tzeng et al. 2004); in most cases, as in the autoregulation of B-function genes that control petal and stamen development in *Antirrhinum majus* (Schwarz-Sommer et al. 1992; Tröbner et al. 1992), they function as heterodimers. Heterodimer formation has been systematically investigated for MADS-domain proteins of *Arabidopsis thaliana* using the yeast 2-hybrid system, and 269 distinct MADS heterodimer species were identified (de Folter et al. 2005). Multimeric complexes have been reported for B-function proteins in *A. majus* (Egea-Cortines et al. 1999) and for several other complexes in *A. thaliana* (Honma and Goto 2001). These studies led to the "floral quartet" model (Theissen and Saedler 2001), which is a combinatorial model that proposes that tetrameric combinations of MADS-domain proteins of defined composition are essential for the specification of floral organ identity.

However, MADS-domain proteins not only interact with each other, they also form functional partnerships with non-MADS-domain proteins. In *Arabidopsis*, several such complexes have been described (Gamboa et al. 2001; Honma and Goto 2001; Pelaz et al. 2001; Fujita et al. 2003; Acevedo et al. 2004; Karlova et al. 2006). In *Antirrhinum*, MIP1, a member of a small family of conserved plant leucine-zipper proteins, can specifically interact with PLE and SEP-like proteins (Davies et al. 1996; Causier et al. 2003). Similarly, a seed-specific histone-fold protein, NF–YB, has been shown to interact with OsMADS18 and OsMADS6 of rice (Masiero et al. 2002).

Although MADS-domain proteins interact both with other MADS-domain proteins and with non-MADS-domain proteins, the factors that govern the selectivity of such interactions—and their biological relevance—are poorly understood. Further insight into this issue is particularly relevant for our understanding of the function of MPF2 in the development of the ICS formation and of its crucial role in male fertility in *P. floridana*.

Here, we describe the identification of several MADS-domain proteins from *Physalis* and *Arabidopsis* that are capable of interacting with MPF2. Among the non-MADS-domain proteins found to interact with MPF2 was a MAGO NASHI-like protein (Boswell et al. 1991; Zhao et al. 1998). In animal systems, such proteins have been shown to function as part of an RNA-processing complex (Zhao et al. 2000; Kataoka et al. 2001; Le Hir et al. 2001; Mohr et al. 2001), and a role in determining fertility has been suggested

Key words: MADS-box, MPF2, PFMAGO, ICS, fertility, *Physalis floridana*, evolution.

E-mail: chaoyhe@mpiz-koeln.mpg.de; saedler@mpiz-koeln.mpg.de.

Mol. Biol. Evol. 24(5):1229–1241. 2007
doi:10.1093/molbev/msm041
Advance Access publication March 5, 2007

for a MAGO NASHI homolog in *Arabidopsis* (Johnson et al. 2004; Pagnussat et al. 2005). Our results will be discussed in an evolutionary context of a proposed network of gene expression machines in plants.

Materials and Methods

Plant Materials

Physalis floridana was grown in greenhouses of the Max-Planck-Institute for Plant Breeding Research (MPIZ), Cologne, Germany.

Isolation of 5′UTR via 5′RACE

The 5′ Untranslated regions (UTRs) of 2 *P. floridana mago nashi* (*PFMAGO*) cDNAs were isolated by rapid amplification of cDNA ends (RACE) using the 5′/3′ RACE Kit (Roche Diagnostics, Mannheim, Germany). The gene-specific primers (SPs) were designed on the basis of the cDNAs obtained from yeast 2-hybrid library screening. For *PFMAGO1*, primer sequences are

SP1: GCATAACGGAGCTTGCCGTCGGGAC,
SP2: CTAAGAACTCGTGCCCGAACTTCCC, and
SP3: GTGACCTACATAGTACCTCAA.

For *PFMAGO2*, primer sequences are

SP1: GCATAACGAAGCTTGCCATCAGGCC,
SP2: CTAAGAACTCATGCCCAAATTTTCC, and
SP3: GTGACCCACGTAATATCTCAGG.

Gene Isolation

Genomic DNAs were isolated from leaves using DIECA (Merck, KGaA, Darmstadt, Germany) buffer. The PFMAGO genes were isolated by polymerase chain reaction (PCR) using the Expand Long Template PCR System (Roche). The primers were designed based on the sequence of the previously obtained full-length PFMAGO cDNAs (see above). The primers are GTGAAGATGGGGGAATTGGAAGAGAATG (forward) and CAAACTGGGTGAATGAGAGGTAGCAAG (reverse) for PFMAGO1 and ATGGGGGAGATGGCAGAGAACGAGGAG (forward) and CGACAACAAATCTCACAAGACATTACAC (reverse) for PFMAGO2.

Promoter Isolation and Analysis

The promoter sequences were obtained by rapid amplification of gDNA ends (RAGE) analysis (Clontech, Laboratories, Inc., Mountain View, CA). Physalis genomic DNA was completely digested with DraI, EcoRV, and ScaI (Roche), respectively, and the fragments were ligated to adaptors using T4 DNA ligase (Roche). PCR was carried out using an adaptor primer and a gene-specific primer. The adaptor and corresponding primers are described in the manual (Clontech), and the gene-specific primers were the same as in the 5′RACE. The promoters were analyzed using the program Credo 1.1–Cis-Regulatory Element Detection Online (http://mips.gsf.de/proj/regulomips/credo.htm). Putative *cis*-acting elements in the promoters were predicted using the plant *cis*-acting regulatory DNA elements (PLACE) database (http://www.dna.affrc.go.jp/htdocs/PLACE; Higo et al. 1999) and MotifFinder (http://motif.genome.jp).

Northern Blot Analysis

Roots, stems, leaves, flowers, and fruits of *Physalis* were harvested and total RNAs were isolated with the total RNA Isolation Reagent Kit (Biomol, Hamburg, Germany). Gene-specific probes (the PCR products from the semiquantitative reverse transcriptase [RT]–PCR) were randomly labeled with Klenow polymerase (Roche) and purified with the High Pure PCR Purification Kit (Roche). Hybridization was done as previously described (He et al. 2002). The filters were then exposed to a Molecular Dynamics Storage Phosphor Screen and the readout processed with a Typhoon 8600 Phosphor Imager (Amersham, Pharmacia Biotech Limited, Little Chalfont, UK). After hybridization, washing, and autoradiography, the *PFMAGO1/2* probes were stripped off in boiling 0.5% Sodium dodecyl sulfate, and the filters were reprobed with radioactively labeled 18S rDNA as loading control.

Semiquantitative RT-PCR

For RT-PCR analysis, total RNAs were isolated from roots, stems, leaves, flowers, and fruits of wild-type *P. floridana* and from leaves and flowers of *MPF2*-knockdown lines (He and Saedler 2005). Samples were treated with DNase I (Roche) to remove contaminating genomic DNA. For the 1st-strand cDNA synthesis, 4 μg of DNase-treated total RNA annealed to oligo $(dT)_{15}$ was used as a template for SuperScript II reverse transcriptase (Invitrogen, Carlsbad, CA) in a 20-μl reaction volume. The forward primer used (CCTGAGGGACTTCGTATCTTC) anneals to both *PFMAGO1* and *PFMAGO2*, but the reverse primers are gene specific (GTGGTCTAAAGAAGAGAGTTCC for *PFMAGO1* and CAAGCAGTGCAGTCTCTTCAG for *PFMAGO2*). All 3 primers were mixed in one reaction tube to quantify the expression of the 2 genes simultaneously. An *ACTIN* cDNA was amplified as an endogenous control (He and Saedler 2005). PCR was performed using the Taq polymerase (Roche), and amplified products were separated on a 1.0% agarose gel. The images were read with a Typhoon 8600 Phosphor Imager (Amersham).

Yeast 2-Hybrid Analysis

The full-length *MPF2* cDNA was cloned into the vector pGBKT7 and transformed into yeast strain AH109. Growth of the transformants on SD/-Trp-His plates indicated that MPF2 could activate the *HIS3* reporter gene on its own (i.e., could self-activate). Deletion of the 46 C-terminal amino acids (the proline-rich and acidic domain) not only abolished self-activation, but also prevented homodimerization and interaction with other MADS-domain proteins. Thus, the truncated version (pGBKT7-MPF2ΔC203) could not be used as bait to screen expression libraries. However, we found that increasing the stringency of the selection (by adding 3-AT [3-amino-1, 2, 4-triazole] and

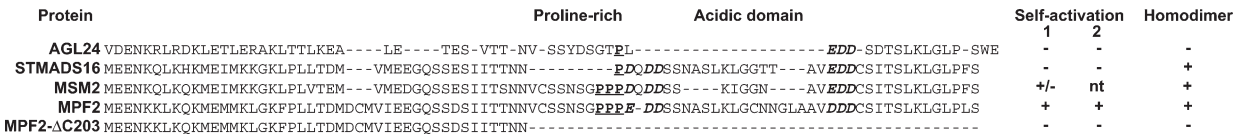

FIG. 1.—Differences in the C-termini of MADS-box proteins belonging to the STMADS16 subclade determine differences in their properties. The gaps were introduced to optimize the alignment of conserved residues. The prolines in the proline-rich domain are shown in bold and underlined. The acidic amino acids in the acidic domain are indicated in bold italics. The ability to self-activate in the 2-hybrid system was revealed by cell growth on SD/-Trp-His (1) and the expression of β-galactosidase, as determined by the development of a blue color in a nonlethal colony assay (2). Symbols + or – indicate growth or no growth (1) or the blue or white phenotype (2); nt is not tested. Homodimer formation (+) was detected as described in Results.

removing Ade) ensured that reporter gene expression due to MPF2 autoactivation was too weak to allow yeast cell growth. Under these conditions, the full-length MPF2 construct could be used as bait to screen 2-hybrid cDNA libraries of *Arabidopsis* and *Physalis* on plates containing SD/-Trp-His-Leu-Ade and 3.0 mM 3-AT.

To confirm the interactions detected, full-length cDNAs were cloned into pGBKT7 and pGADT7, respectively. In cases where proteins showed autoactivation (AP1, SEP1, SEP2, and SEP3), C-terminal deletion derivatives were used in bait constructs. To confirm MADS-dimerization (outlined in table 2), single transformations of bait into yeast strain Y187 and prey into strain AH109 carried out, and different combinations of bait and prey were brought together by mating the 2 strains. Cotransformations were performed to verify the MADS–PFMAGO interactions (see fig. 2). Subsequent to these operations cells were plated on medium-stringency plates (SD/-Trp-His-Leu) and high-stringency plates (SD/-Trp-His-Leu-Ade and 3.0 mM 3-AT), respectively. The media were prepared according to the recommendations in the Clontech manuals. Yeast cells were incubated in a growth chamber at 28 °C for 2–5 days. Yeast manipulations were performed following standard procedures (Clontech). The nonlethal β-galactosidase assay was performed as described by Duttweiler (1996).

cDNA Library Construction and Screening

Total RNAs from stems, leaves, flower buds (different developmental stages), mature flowers and young fruits (with calyx) of *Physalis* were separately isolated and mixed. The cDNA was synthesized using either oligo(dT) or random primers. The library was made as described in the Clontech manual. The oligo (dT)-primed library contained 3×10^8 cells/ml and the randomly primed library had 2.2×10^8 cells/ml.

An *Arabidopsis* library (Sommer H, Masiero S, unpublished data) and the *Physalis* libraries were screened using a bait vector carrying the full-length coding region of an *MPF2* cDNA. The isolated *Physalis Mago Nashi* cDNAs *(cPFMAGO1* and *cPFMAGO2*) were used to construct new baits to screen the *Physalis* libraries. After mating, the yeast cells were plated on high-stringency plates (SD/-Trp-His-Leu-Ade plus 3.0 mM 3-AT) and kept at 28 °C for 5–10 days. Colonies larger than 2 mm were picked and re-streaked onto 2 selective plates and grown at 28 °C for 1 week. One plate was subjected to the nonlethal β-galactosidase assay, whereas the other served as storage plate for PCR. The blue colonies recovered were further characterized by PCR sequencing analysis according to Ling et al. (1995).

Sequencing Analysis

All genomic and cDNA PCR fragments were fractionated on 1.0% agarose gels and purified with the Highly Pure PCR Product Purification Kit (Roche) and then cloned into the pGEM T-easy vector (Promega, Madison, WI). The plasmids were extracted with the Miniprep Plasmid Purification Kit (Qiagen, Hilden, Germany). Yeast clones were characterized by direct PCR purification and sequencing analysis. Sequencing was performed at the Automatic DNA Isolation and Sequencing Unit of the MPIZ, Cologne, Germany. The nucleotide sequences reported were deposited in the National Center for Biotechnology Information database under the accession numbers EF205415 (genomic sequence of *PFMAGO1*), EF205416 (genomic sequence of *PFMAGO2*), EF205417 (cDNA sequence of *PFMAGO1*), and EF205418 (cDNA sequence of *PFMAGO2*).

Results

Phylogenetic reconstructions of the MADS-box gene family have revealed the existence of many subclades of functionally related members (Becker and Theissen 2003). However, members of some of these subclades fulfill quite diverse functions. For example, STMADS16, AGL24, and MPF2 are orthologous proteins from different species that belong to the STMADS16 subclade (He and Saedler 2005), but they differ markedly in function (Garcia-Maroto et al. 2000; Yu et al. 2004; He and Saedler 2005). This may be attributed to sequence divergence between them at their C-terminal ends (fig. 1). For instance, MPF2 from *P. floridana* has a proline-rich, acidic domain at its C-terminus, which is missing in AGL24 from *Arabidopsis thaliana*, whereas STMADS16 from *S. tuberosum* lacks the proline-rich segment. The C-terminal region of MSM2 from *S. macrocarpon* on the other hand is very closely related to that of MPF2 with some small deletions in the acidic domain. The differences in domain organization suggest that these proteins play different roles in transcription activation and may form complexes with (partially) distinct sets of partners. In the present study, we have used the yeast 2-hybrid system to identify proteins with which MPF2 can interact.

The C-Domain of MPF2 is Involved in Autoactivation and Is Essential for Homodimer Formation in Yeast

Full-length cDNAs encoding MPF2 were introduced into yeast 2-hybrid prey and bait vectors (Materials and

Table 1
MADS Interactors of MPF2 from the *Arabidopsis* and *Physalis* Library Screens

	Total	AP1	SEP1	SEP3	SEP4	AGL6	AG	SOC1
Arabidopsis	17	3	1	4	8	0	0	1
Physalis	34	2	4	15	0	8	4	1
	Total	MPF3	SEP1-L	SEP3-L	SEP4-L	AGL6-L	AG-L	SOC1-L

NOTE.—L is abbreviated from Like.

Methods), respectively, to check its intrinsic transcriptional activating properties and its potential toxicity in yeast. All transformed yeasts grow normally on tryptophan-deficient (bait) or leucine-deficient (prey) plates, indicating that the transgene is not toxic to yeast. Yeast cells expressing *AGL24* from *Arabidopsis* or *STMADS16* from *S. tuberosum* fail to grow on histidine-deficient plates (SD/-Trp-His), whereas cells expressing *MSM2* from *S. macrocarpon* or *MPF2* from *P. floridana* grow slowly on the same medium. These findings indicate that whereas AGL24 and STMADS16 are not self-activating, MSM2 and MPF2 show differing self-activation capacities (fig. 1). These differences might be related to C-terminal sequence divergence. To test this idea, the putative transactivating region (the 46 amino acids that comprise the proline-rich and acidic domains) was deleted from MPF2 and, as expected, the resulting truncated derivative (MPF2ΔC203) no longer activated the *HIS3* reporter gene (fig. 1).

The ability of these proteins to form homodimers was investigated as well. Clearly, STMADS16-like proteins from Solanaceae can homodimerize, but the truncated version of MPF2 neither forms homodimers nor interacts with full-length MPF2. AGL24, the *Arabidopsis* ortholog of MPF2 and STMADS16 (Masiero et al. 2004; He and Saedler 2005), also cannot form homodimers (fig. 1). This is very likely due to the divergence in the C-terminal region of AGL24 with respect to its solanaceous orthologs.

Deletion of the C-terminal region of MPF2 abolishes its function, as judged by the failure of the truncated version to homodimerize and autoactivate (fig. 1). For this reason, MPF2ΔC203 cannot be used to search for MPF2-interacting proteins using 2-hybrid technology. Therefore, full-length MPF2 cDNA was used as bait to screen an expression library of *Arabidopsis* and *Physalis*, respectively, for interacting proteins. To prevent the growth of indicator cells due to low-level self-activation of the bait, selection was performed under high-stringency conditions (see Materials and Methods).

Screening of cDNA Expression Libraries

Because AGL24 and MPF2 are orthologs, we expected that they would interact with similar sets of interacting proteins. Therefore, cDNA expression libraries from both *Arabidopsis* and *Physalis* were screened with full-length MPF2 as bait in the yeast 2-hybrid system (for details see Materials and Methods).

A total of 95 positive colonies obtained from the *Arabidopsis* library were analyzed further, leading to the identification of 5 different MADS-box genes: *SOC1*, *AP1*, *SEP1*, *SEP3*, and *SEP4* (table 1).

These 5 include some, but not all, of the proteins known to interact with AGL24 (de Folter et al. 2005). Our failure to isolate, for example, AG and AGL6 in this screen might have been a consequence of the relatively small number of colonies examined in detail or of the heterologous nature of the system.

Two different *Physalis* cDNA expression libraries were constructed (Materials and Methods) and screened. Screening of these 2 libraries with MPF2 as bait yielded SOC1-, AP1- (termed MPF3; He et al. 2004), SEP1-, SEP3-, AG-, and AGL6-like clones (table 1). Interestingly, although MPF2 can interact with SEP4 from *Arabidopsis* (table 1), no genes for SEP4-like proteins could be isolated from the *Physalis* libraries in the yeast 2-hybrid system.

Verification of Interactions in Yeast

In order to confirm the interactions identified in the library screens, both bait and prey constructs were independently transformed into the yeast strains Y187 and AH109,

Table 2
Reciprocal Interactions among MPF2-Like Proteins and Their *Arabidopsis* Interactors

	AGL24	STMADS16	MSM2	MPF2	MPF2ΔC203	AP1ΔC196	SEP1ΔC168	SEP2ΔC168	SEP3ΔC171	SEP4	SOC1	PGBKT7
AGL24	−	−	−	−	−	+	++	−	++	++	++	−
STMADS16	−	++	++	++	−	+	++	−	++	++	++	−
MSM2	−	++	++	++	−	+	++	−	++	++	++	−
MPF2	−	++	++	++	−	+	++	−	++	++	++	−
AP1	+	+	+	+	−	+	+	−	+	++	+	−
SEP1	++	++	++	++	−	++	−	−	−	++	++	−
SEP2	−	−	−	−	−	−	−	−	−	++	++	−
SEP3	++	++	++	++	−	+	−	−	−	++	++	−
SEP4	+	+	+	+	−	++	−	−	−	++	−	−
PGADT7	−	−	−	−	−	−	−	−	−	−	−	−

respectively. In cases of self-activation, C-terminally truncated versions of the respective proteins were used as baits. The yeast strains were mated and subjected to the nonlethal β-galactosidase assay (Materials and Methods).

Most of the putative MPF2 interactors from *A. thaliana* are known to heterodimerize with AGL24 (de Folter et al. 2005). Because SEP1, SEP2, SEP3, and AP1 can self-activate, the corresponding bait constructs encoded C-terminally truncated versions referred to as SEP1ΔC168, SEP2ΔC168, SEP3ΔC171, and AP1ΔC196, respectively. In addition to lacking the ability to self-activate, SEP2ΔC168 and MPF2ΔC203 have also lost their capacity to homo- or heterodimerize (table 2). AGL24 from *Arabidopsis* did not form homodimers nor did it interact with orthologs from solanaceous plants, but it clearly heterodimerized with AP1, SEP1, SEP3, SEP4, and SOC1. A strain containing an empty vector as a negative control was unable to grow on plates lacking histidine.

The solanaceous orthologs MPF2, STMADS16, and MSM2 (He and Saedler 2005) formed dimers with each other, but not with AGL24, in addition, all of them heterodimerized with SOC1, AP1, SEP1, SEP3, and SEP4. They thus bind to a subset of the MADS-domain proteins that interact with AGL24 in *Arabidopsis*, confirming the results of the *Arabidopsis* library screen.

Putative Non-MADS-Domain Proteins That Interact with MPF2

As mentioned above, MADS-domain proteins can also interact with non-MADS-domain proteins (see Introduction and supplementary table 1, Supplementary Material online), and indeed, in addition to the 34 MADS-box clones described in the previous section, 24 clones homologous to *mago nashi* were isolated in our screens for MPF2 interactors.

The gene *mago nashi* was first discovered in *Drosophila* (Boswell et al. 1991; Newmark and Boswell 1994) and suggested to play a fundamental role in the establishment of polarity and germ cells during embryonic development.

The 1st *mago nashi* homolog found in plants was isolated and characterized from *Oryza sativa* (Swidzinski et al. 2001) and *mago nashi* mutations were found to cause sterility in *A. thaliana* (Johnson et al. 2004; Pagnussat et al. 2005).

Because MPF2 also affects male fertility (He and Saedler 2005), we decided to undertake a detailed molecular characterization of PFMAGO and its interaction with MPF2.

Confirmation of the MPF2–PFMAGO Interaction in Yeast

Cloning and sequencing of full-length cDNAs for *PFMAGO* revealed 2 different but closely related products termed c*PFMAGO1* and c*PFMAGO2*. Both cDNAs were cloned into bait and prey vectors, respectively. Analysis of yeast transformants suggested that neither of the *MAGO NASHI* homologs could activate *lacZ* and *HIS3* reporter genes on its own and neither was toxic to yeast (data not shown). After cotransformation, yeast AH109 cells containing the cDNA constructs *MPF2* and *PFMAGO1* or *MPF2* and *PFMAGO2* as bait or as prey, respectively, were plated on SD/-Trp-Leu-His-Ade, plus 3.0 mM 3-AT. Transformed cells carrying these bidirectional combinations were recovered (fig. 2*A*), and when subjected to the nonlethal β-galactosidase assay these cells turned blue (fig. 2*B*), thus confirming the results of the library screen albeit a much weaker interaction is observed using MPF2 as well as STMADS16 as bait (fig. 2). The reason for this is not clear yet. Moreover, MPF2 displays similar affinities for PFMAGO1 and PFMAGO2. STMADS16, the MPF2 ortholog from *S. tuberosum*, can also interact with both PFMAGO proteins. However, not all MADS-domain proteins are able to interact with the 2 PFMAGO proteins. MPF1 and STMADS11, close homologs of MPF2 and STMADS16, respectively (He and Saedler 2005), show no interaction with PFMAGO (fig. 2). Therefore, the interaction of MPF2 with the 2 PFMAGO proteins seems to be quite specific.

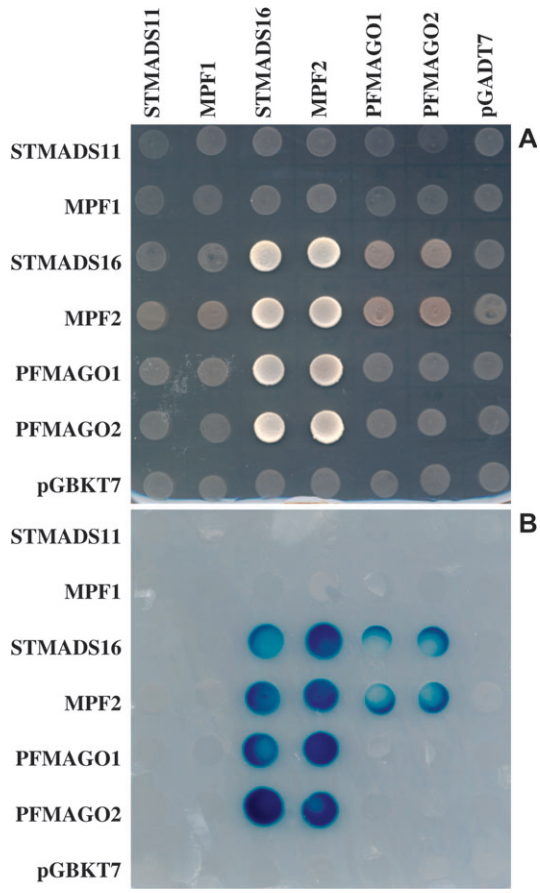

FIG. 2.—Confirmation of MPF2–PFMAGO interactions. (*A*) Cell growth in the yeast 2-hybrid system on a high-stringency selective plate (SD/-Trp-His-Leu-Ade and 3.0 mM 3-AT). (*B*) Nonlethal β-galactosidase test to confirm the interactions. The expressed prey proteins are indicated above and the bait proteins to the left of the panels.

In addition, these results demonstrated that neither PFMAGO1 nor PFMAGO2 can form homodimers, and they corroborate the previous findings regarding the ability of MPF2 and STMADS16, respectively, to heterodimerize. Furthermore, MPF1 and STMADS11 neither homodimerize nor do they heterodimerize with MPF2 or STMADS16 (fig. 2).

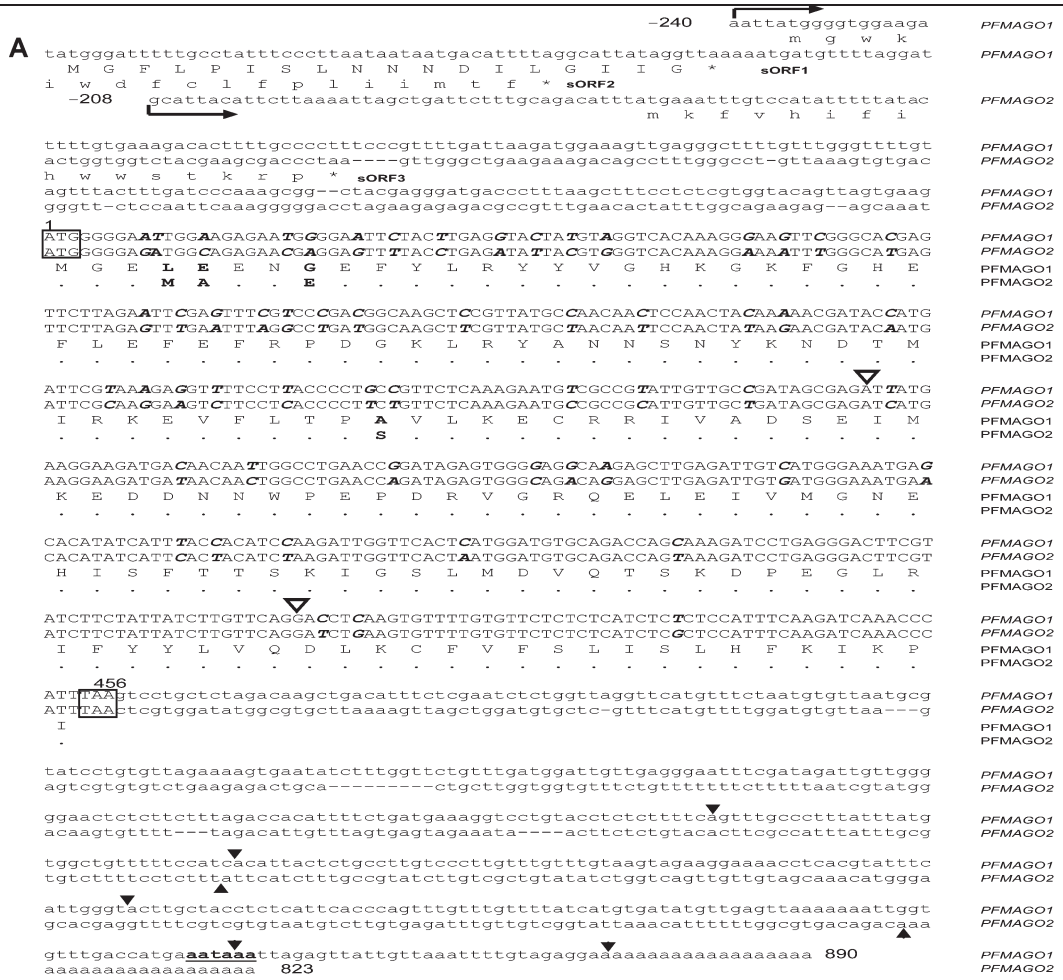
A
B
C
PFMAGO1
PFMAGO2
sORF1
sORF2
sORF3
A. thaliana
O. sativa
P. patens
C. elegans
D. melanogaster
H. sapiens
M. musculus
Arabidopsis homolog
Rice homolog
-1560
5100
-1861
6100
-2000
1250
-2000
3560

Both *PFMAGO1* and *PFMAGO2* were further characterized molecularly.

Molecular Characterization of *PFMAGO1* and *PFMAGO2* Gene Products

5′RACE was used to obtain full-length cDNAs. The longest *PFMAGO1* cDNA comprises 1130 bp, whereas the equivalent *PFMAGO2* sequence is 1031-bp long. Both encode polypeptides of 151 amino acid residues (fig. 3*A* and *B*). Sequence comparison indicated that the coding regions shared 84% identity (56 single-nucleotide differences in 453-bp coding region) at the nucleotide level, whereas their protein products are 97.4% identical (4 differences in 151 amino acid residues; fig. 3*A* and *B*). Sequence comparison showed that the PFMAGOs shared 74–93% identity with other MAGO NASHI homologs from species as different as moss and animals (fig. 3*B*). With the exception of the N-terminal region, which is highly variable in composition and length, these homologs are all highly conserved. Three out of the 4 amino acid residues that differ between the 2 *Physalis* proteins are located in the variable region. The conservation of these proteins among distant taxa (fig. 3*B*) suggests that they have a fundamental function.

Major sequence divergence between the 2 *PFMAGO* mRNAs (fig. 3*A*) was observed in their 5′UTRs and 3′UTRs. UTRs are believed to contain regulatory signals that can act at both transcriptional and posttranscriptional levels. The 5′UTR of *PFMAGO1* encodes 2 small open reading frames (sORFs; 18 amino acids, respectively): sORF1 is in frame and sORF2 out of frame with respect to the main coding region. The 5′UTR of *PFMAGO2* also contains a 3rd, out of frame, sORF3 (16 amino acids; fig. 3*A*). Whether any of these sORFs in the UTRs of the *PFMAGO* RNAs has a regulatory role is not known.

Polyadenylation is an important step in the maturation of mRNAs, and the site of polyA addition is determined by certain signal sequences in the 3′UTR. As indicated in figure 3*A*, only one putative polyadenylation signal sequence (AATAAA) could be recognized in *PFMAGO1*, although the cDNAs recovered revealed that at least 5 polyadenylation sites are used; *PFMAGO2* has 2 such sites as deduced from the different cDNA sequences isolated.

The 5′UTR and 3′UTR of both *PFMAGO* cDNAs are very different in sequence and the promoter and intron sequences are also diverged (see below), which suggest that 2 *PFMAGO* genes occur in the genome of *P. floridana*.

Gene Structure

To determine the exon–intron structure of the 2 *PFMAGO* genes, long-template PCR was used (Materials and Methods). The gene-specific primers were derived from the cDNAs. The 5.1- and 6.0-kb fragments were obtained from the *P. floridana* genome, corresponding to *PFMAGO1* and *PFMAGO2*, respectively. The 2 genes have similar structures, comprising 3 exons—like their *Arabidopsis* and rice homologs. The intron lengths are highly variable (fig. 3*C*). For example, the 1st intron of *PFMAGO1* is 73-bp long, whereas that of *PFMAGO2* is 967-bp long. Although the genes differ in overall length in the different plant species, the intron positions are conserved (fig. 3*B* and *C*). However, the *PFMAGO* gene structures differ substantially from those of their homologs in nonplant organisms (supplementary table 2, Supplementary Material online).

Promoter Analyses

Promoter regions of *PFMAGO1* and *PFMAGO2* were isolated using RAGE (Materials and Methods). The *PFMAGO1* fragment obtained covers 1560 bp and that of *PFMAGO2* is 1861-bp long. The 1st nucleotide of the ATG start codon was defined as position 1. The putative transcription initiation sites, indicated by arrows in figure 4, were deduced from the longest 5′UTR obtained by 5′RACE (fig. 3*A*). Transcription appears to initiate in *PFMAGO1* at around position −240 and at position −208 in *PFMAGO2*. The promoter region upstream of the ATG start codon shows about 44% sequence conservation between the 2 genes. The difference is partly attributable to an 835-bp insertion in the *PFMAGO2* promoter, extending from position −1054 to position −1889. DiAlign analysis (http://mips.gsf.de/proj/regulomips/credo.htm) recovered a patchwork of 11 homology regions distributed along the 2 promoters (fig. 4). The combined length of these motifs is 320 bp and these sequences show 70% identity between the genes, whereas the intervening variable regions, which constitute the majority of the promoter region, show only 36% identity.

Interestingly, neither Align ACE (Roth et al. 1998) nor Motif sampler (Thijs et al. 2001) detected any conspicuous

←

FIG. 3.—Molecular characterization of the *PFMAGO* genes in *Physalis*. (*A*) Alignment of the *PFMAGO* cDNA sequences and their deduced proteins products. The coding regions are shown in upper case, whereas UTR sequences in lower case. The differences in the coding regions of the 2 genes are indicated in bold italics. The arrows indicate the putative transcription initiation sites. The initiator ATGs are boxed and the first base set as position 1. Differences in amino acid residues encoded by the major ORFs are shown in bold, whereas amino acid identities are shown as dots for PFMAGO2. The sequences of the in-frame sORFs in the 5′UTR and the major ORFs are depicted in upper case, whereas the out-frame sORFs are in lower case. The stop codons are boxed. A putative polyadenylation signal in the 3′UTR of *PFMAGO1* is shown in bold and underlined. The filled triangles indicate the positions of the functional polyA sites. The empty triangles indicate intron positions. (*B*) Comparison of MAGO NASHI sequences from different species. The variable region at the N-terminus of MAGO NASHI is boxed. Sequence differences are underlined. The arrows indicate intron positions in plant *MAGO NASHI* genes. The sequences shown here are PFMAGO1 and PFMAGO2 from *Physalis floridana*, which were isolated in this study, At1g02140 from *Arabidopsis thaliana*, ABA97757 from *Oryza sativa*, AAW78461 from *Physcomitrella patens*, NP_476636 from *Drosophila melanogaster*, CAB03239 from *Caenorhabditis elegans*, AAH10905 from *Homo sapiens*, and AK008200 from *Mus musculus*. (*C*) Structures of selected plant *MAGO NASHI* genes. *PFMAGO1* and *PFMAGO2* from *P. floridana* were isolated in this study. The *Arabidopsis* homolog At1g02140 and the rice homolog DP00001 were included for comparison. The open boxes indicate the exons and the black lines represent the promoters, introns, and UTRs. The first nucleotide of ATG was set as 1.

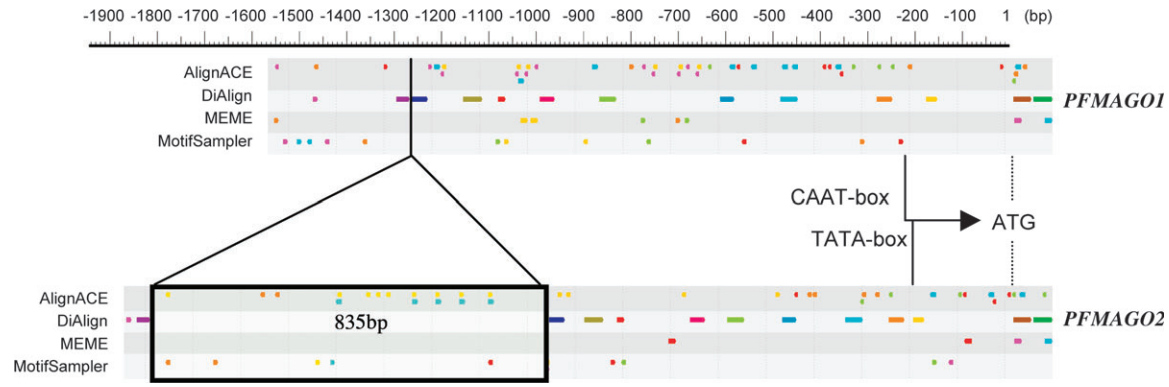

FIG. 4.—Promoter analysis of the 2 *PFMAGO* genes. The colored boxes indicate regions of homology and motifs identified by DiAlign analysis. The (gray) gaps between the boxes show highly variable regions. The arrow indicates the putative transcription initiation sites. The 835-bp insertion in the *PFMAGO2* promoter is highlighted. The positions of the initiator ATG is indicated by the dashed lines and the first nucleotide of this codon is taken as 1.

conserved motifs within the patchwork of the 11 homology regions found by DiAlign analysis (fig. 4).

An independent search for motifs known to act as *cis*-regulatory elements in plants, using the PLACE database (Higo et al. 1999), yielded (besides basic motifs required for most promoters like CAAT and TATA boxes) a large number (102) of motif types in both promoters: 55 of these motif types are present in both promoters, whereas 27 are specific for *PFMAGO1* and 20 for *PFMAGO2*. A selection (36 out of 102) of interesting *cis*-elements is listed in supplementary table 3 (Supplementary Material online), together with their distribution in the 2 promoters. Because many transcription factors could potentially recognize these motifs, different hormone signaling pathways, stress conditions, and light and circadian rhythm might control the expression of the *PFMAGO* genes. *Cis*-acting elements were also sought using MotifFinder (http://motif.genome.jp). With the cutoff score set to 85 (default), 9 different motif types were found in the *PFMAGO1* promoter and 6 in the *PFMAGO2* promoter: 6 of these are shared by both promoters, although the numbers of each motif type differ between the 2 (data not shown).

These analyses demonstrated that the 2 promoter regions are quite divergent but have retained certain stretches of conserved sequences and motif types, which might indicate different but overlapping expression profiles for these 2 genes.

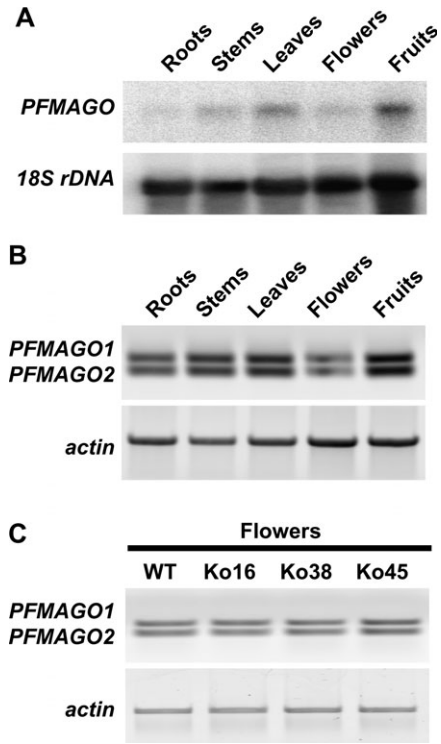

FIG. 5.—Expression of the *PFMAGO* genes in *Physalis*. (*A*) Expression pattern of *PFMAGO* in different organs. Northern analysis was performed using total RNAs from the tissues indicated above the panel. 18S rDNA was used as an RNA loading control. (*B*) Coregulation of *PFMAGO1* and *PFMAGO2*. Semiquantitative RT-PCR analysis was carried out using total RNA from the indicated tissues. The upper panel shows *PFMAGO1* and *PFMAGO2* (from top to bottom). The lower panel shows *ACTIN* expression in the corresponding lane as a control. (*C*) MPF2 does not affect *PFMAGO* expression in *Physalis*. Semiquantitative RT-PCR analysis was carried out using total RNA from wild-type and *MPF2* RNAi *Physalis* flowers. The upper panel shows *PFMAGO1* and *PFMAGO2* (from top to bottom). The lower panel shows *ACTIN* expression in the corresponding lane as a control.

Tissue-Specific Expression of PFMAGO1 and PFMAGO2

The *MAGO NASHI* homologs in rice and *Arabidopsis* show widespread expression in many different tissues (Swidzinski et al. 2001; Zimmermann et al. 2004). This is also true for *Physalis*. Total RNA was isolated from root, stem, leaves, flowers, and fruits and analyzed in Northern blot experiments. Clearly the *PFMAGO* genes are expressed in all tissues tested, though at different levels (fig. 5*A*). The strongest expression was observed in leaves and fruits. Weak signals were detected in root, stem, and flower. As their RNA products are indistinguishable on northern blots, gene-specific primers were designed to discriminate between the mRNAs and determine their individual levels via RT-PCR.

Two products could be amplified corresponding to *PFMAGO1* and *PFMAGO2*. Surprisingly, the ratio of their intensities seemed to be similar in all tissues (fig. 5*B*), suggesting that *PFMAGO1* and *PFMAGO2* are regulated coordinately.

Because MPF2 is a transcription factor and can interact with PFMAGO in yeast, the *PFMAGO* gene might itself be a target of MPF2. *MPF2* RNAi plants show a reduced level of

MPF2 mRNA (He and Saedler 2005) and thus allow us to test this possibility. Total RNAs were isolated from leaves and flowers of wild-type and RNAi lines, and the levels of *PFMAGO* transcripts in these *MPF2* RNAi lines were measured by semiquantitative RT-PCR. In none of the transgenic *MPF2* RNAi lines was *PFMAGO* gene expression altered relative to wild type, either in floral tissues (fig. 5*C*) or in leaves (data not shown). Therefore, MPF2 does not regulate the *PFMAGO* genes at the transcriptional level.

Identification of PFMAGO-Interacting Factors

Factors that interact with MAGO NASHI have been described in animal systems (Zhao et al. 2000; Kataoka et al. 2001; Le Hir et al. 2001; Mohr et al. 2001), but nothing is known about MAGO NASHI-interacting proteins in plants.

Both PFMAGO proteins were therefore used as baits in the yeast 2-hybrid system to screen *Physalis* cDNA expression libraries for interacting factors. In all, 574 clones were rescued and sequenced. Half the candidates were either single cases or proteins of unknown function; the other major fraction included components of different gene expression machines. Based on these results, PFMAGO can interact with ribosomal proteins, translation initiation, and elongation factors and a large number of putative transcription factors. However, no MADS-box transcription factors have yet been found among this last class of candidate interactors (supplementary table 4, Supplementary Material online). Similar observations were made in *Physalis* library screens using MPF2 as bait, which did not yield MPF2 although MPF2 can form homodimers. The reason for this is unknown. A possible explanation could be the low frequency of full-size *MPF2* cDNAs in the libraries. Truncated MPF2 versions, especially from the C-domain (fig. 1) abolish MPF2 homo- or heterodimer formation.

Strikingly, the major interacting protein identified (accounting for ca. 20% of the colonies rescued and sequenced) was an RNA-binding protein that is known to bind MAGO NASHI in animal systems. Blast searches revealed that all 118 sequences coded for homologs of Y14 or Tsunagi (Hachet and Ephrussi 2001; Mohr et al. 2001), suggesting formation of a PFMAGO–Y14 complex also in plants. As in animals (Le Hir et al. 2001), PFMAGO could function as a molecular integrator of different gene expression machines. The extent of this network, however, remains to be clarified.

Discussion

The ICS seen in *P. floridana* was previously shown to result from heterotopic expression of the MADS-box gene *MPF2* with respect to its ortholog *STMADS16* of *S. tuberosum*, a species in which the sepals remain small throughout flower and fruit development (He and Saedler 2005, 2007). Moreover, MPF2 is not only involved in ICS formation, but is also required for male fertility. RNAi-mediated *MPF2* knockdown in *P. floridana* results in male sterility (He and Saedler 2005).

Our knowledge of the molecular mechanisms that underlie these 2 processes in solanaceous species is rather rudimentary. Therefore, a comparison with the extensively studied *Arabidopsis* ortholog AGL24 may provide useful insights.

In wild-type *Arabidopsis*, AP1 restricts *AGL24* expression to vegetative tissues and prevents its expression in floral organs (Yu et al. 2004). The *ap1* mutants form leaf-like sepals (Mandel et al. 1992), as indicated by their leaf- or bract-like stellate trichomes. Concomitantly a change in organ size is also observed. These features of *ap1* mutants are very likely to be due to ectopic expression of *AGL24*, as sepals also become leaf-like in transgenic *Arabidopsis* plants that overexpress *AGL24* (He et al. 2004; Yu et al. 2004).

AGL24 and MPF2 differ at their C-terminal ends and are thus expected to differ somewhat in their properties. Indeed, although MPF2 shows a propensity to self-activate in yeast, AGL24 shows no such tendency. Moreover, MPF2 forms homodimers in the yeast 2-hybrid system and interacts with its orthologs from solanaceous plants, but not with AGL24; in our hands, AGL24 itself does not homodimerize. This latter finding is consistent with a report by Takemura et al. (2004) (abstract T01-014 of 15th International Conference on Arabidopsis Research 2004, Berlin, page 93, also see www.arabidopsis.org/news/15Arab Abstract.pdf) but is in conflict with the results reported recently by de Folter et al. (2005), who confirmed a lack of autoactivation, but did observe homodimerization of AGL24. Furthermore, they suggest in their "Flower Induction and Flower Formation Network" that AGL24 interacts "indirectly"—through SOC1—with the 2 isoforms of SEP4 (de Folter et al. 2005). In the experiments presented here AGL24, however, was found to interact "directly" with both SEP4 and SOC1.

In any case, MPF2 interacts with a broad subset of the proteins that bind to AGL24, including SOC1, AP1, SEP1, SEP3, AG, and AGL6. Orthologs of all MPF2-interacting *Arabidopsis* MADS-box proteins were recovered from the *Physalis* cDNA expression libraries—with the exception of SEP4, even though MPF2 shows the capacity to interact with SEP4 in *Arabidopsis*. Our inability to identify a *Physalis SEP4* homolog in the yeast 2-hybrid system may indicate that it is represented at very low levels in our cDNA libraries: alternatively, *Physalis* may not possess or even express such a gene.

In the following, the Physalis factors found to interact with MPF2 will be discussed with respect to their possible roles in ICS formation and male fertility.

The Role of MPF2 and Its Interacting Proteins in ICS Formation

According to the "floral quartet" hypothesis, a tetrameric complex consisting of 2 MPF3 (AP1-like, AP1-L) and 2 SEP-like (SEP-L) molecules is thought to specify sepal organ identity (fig. 6). Unfortunately, no *mpf3* mutant affecting sepal organ identity has yet been described in *Physalis*. On the other hand, however, the size of the lantern can vary depending on the amount of MPF2 available in sepal tissue, as suggested by the phenotypes of *MPF2* RNAi transgenic plants (He and Saedler 2005).

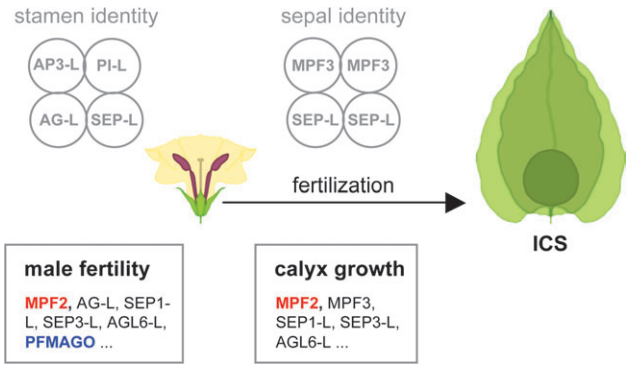

FIG. 6.—Roles of MPF2 in flower development of *P. floridana*. Stamen and sepal/calyx (highlighted in purple and green, respectively) are the floral organs affected by MPF2. The MPF2 (red) interacting proteins so far identified are listed in the boxes and tentatively assigned to one or the other process. PFMAGO is highlighted in blue. L is abbreviated from Like.

Unlike the situation in *Arabidopsis* (see above), sepal identity and sepal size seem not to be linked in *Physalis*. As we showed previously, calyx growth in *Physalis* depends on sepal cell division controlled by MPF2 in combination with plant hormones (He and Saedler 2007). Specifically, cytokinins facilitate import of MPF2 into the nucleus, ultimately resulting in the production of small cells, which then enlarge in response to gibberellins. Other MPF2-interacting MADS-domain proteins, like MPF3, SEP1-L, SEP3-L, AGL6-L, and others (fig. 6), may contribute to this process, but this issue remains to be clarified.

MPF2 and Its Possible Role in Male Fertility

The ABC model of flower development suggests that B- and C-functions together confer stamen organ identity; according to the "floral quartet" model, this is accomplished by combinations of AP3, PI, AG, and SEP proteins. However, many gene products, including MADS-domain proteins, are required for the primary function of the anthers, that is, male fertility. In *Arabidopsis*, AGAMOUS is essential for stamen and carpel organ identity. In *Antirrhinum*, however, a duplication of the ortholog of *AGAMOUS* occurred and was followed by subfunctionalization of the resulting *PLENA* and *FARINELLI* genes (Causier et al. 2005). Although PLENA continues to provide the organ identity function, its paralog FARINELLI adopted a new function. The *farinelli* mutants show no homeotic transformation of the male organ, but nevertheless are male sterile (Davies et al. 1999). Currently there is no evidence for AG-L duplication in *Physalis*. Therefore, the *Physalis* AG-L isolated might provide both functions, conferring organ identity in whorls 3 and 4 and in addition ensuring male fertility by interacting with MPF2.

In tomato (*Solanum lycopersicum*) a different MADS-box protein, TM29, appears to be involved in establishing fertility. Down-regulation of this *SEP4* ortholog leads to a complex phenotype including sterility (Ampomah-Dwamena et al. 2002; Hileman et al. 2006). Although MPF2 interacts with SEP4 from *A. thaliana*, no such MADS-box protein was isolated from our *Physalis* cDNA libraries, which might indicate that MPF2 acts like a SEP4-like protein in this species. However, this possibility needs to be more rigorously tested. Therefore, the question of how MPF2 might affect male fertility in combination with other MADS-domain interacting proteins must remain open.

The striking finding that a non-MADS-domain protein, PFMAGO, a homolog of MAGO NASHI, interacts with MPF2 opens a new approach that might allow us to shed more light on MPF2's function in male fertility.

The gene *mago nashi* (meaning "no grandchildren" in Japanese) was first identified as a strict maternal effect gene in *Drosophila*, where it is required for the formation of the embryonic axes and for germ-cell determination (Boswell et al. 1991; Newmark and Boswell 1994; Micklem et al. 1997; Newmark et al. 1997). Its *Caenorhabditis* homolog *mag-1* is required for germline sexual switching and embryogenesis (Li et al. 2000; Kawano et al. 2004). Furthermore, MAGO NASHI has been found to be an integral part of the exon–exon junction complex (EJC) assembled on RNAs 20 nucleotides upstream of exon–exon junctions (Kataoka et al. 2001; Bono et al. 2004). It always functions together with an RNA-binding protein, known as Y14 in *Xenopus* (Kataoka et al. 2000), RBM8A in humans (Zhao et al. 2000), and Tsunagi in *Drosophila* (Mohr et al. 2001), a protein that shuttles between nucleus and cytoplasm (Hachet and Ephrussi 2001, 2004; Kim et al. 2001). The MAGO NASHI–Y14 interaction is highly specific and highly conserved (Zhao et al. 2000; Kataoka et al. 2001; Le Hir et al. 2001; Mohr et al. 2001) and has been confirmed by the determination of the crystal structure of the *Drosophila* Mago nashi–Y14 complex (Shi and Xu 2003) and the 3-dimensional architecture of the EJC core (Stroupe et al. 2006). The heterodimer serves as a core component of the EJC (Lau et al. 2003; Shi and Xu 2003; Tange et al. 2005; Stroupe et al. 2006) and remains associated with the exon junctions during and after export from the nucleus; in the cytoplasm, the complex serves to control mRNA localization, as has been shown for *oskar* mRNA in the *Drosophila* embryo (Micklem et al. 1997; Newmark et al. 1997; Mohr et al. 2001; Hachet and Ephrussi 2004). In addition, MAGO NASHI has been shown to be a component of the nonsense-mediated mRNA decay (NMD) pathway that acts as a quality control on mRNAs in the cytoplasm and its association with Y14 is essential for this function as well (Fribourg et al. 2003). MAGO NASHI, therefore, appears to serve as a molecular link between gene expression machines that act in different processes, and—most intriguingly—play a role in germ cell development. MAGO NASHI homologs in plants might have similar functions.

Transcription and RNA splicing is linked as shown in animals (Heyd et al. 2006). We report here, for the first time in plants, on an interaction between a transcription factor (MPF2) and a PFMAGO and also show that PFMAGO robustly binds to an Y14-like protein and some translation-related factors from *Physalis*. The specificity of the MPF2–PFMAGO and PFMAGO–Y14 homolog interactions in *Physalis* also suggests the existence of an interaction network that couples transcription, RNA processing, and possibly translation in plants. Support for this assumption comes from the large number of other putative transcription

factors and translation factors that interact with PFMAGO in *P. floridana*. Although transcription and RNA processing occur in the nucleus, translation takes place in the cytoplasm. It seems highly unlikely that MPF2 forms part of the translation machinery, but PFMAGO most probably participates in transcription, RNA splicing, RNA quality control, and translation. Therefore, PFMAGOs may well serve as a shuttle between the different gene expression machines, as their homologs do in animal systems.

MPF2's role in male fertility in *Physalis* was revealed by the male-sterile phenotype observed in *MPF2* RNAi knockdown plants. Interestingly, in *Arabidopsis*, *mago nashi* mutants show a "haploid disruptions" (*hapless*) phenotype. Defects are observed in pollen tube growth (Johnson et al. 2004) and in female reproductive organs in which embryo development arrests at various stages (Pagnussat et al. 2005). By analogy, the PFMAGOs might also influence pollen or embryo development in *Physalis*.

The dual functions of MPF2, promoting cell division in the calyx upon fertilization and determining male fertility, are highlighted in figure 6. Elucidation of the molecular details, however, will obviously require further work.

Apparently, the protein interacting networks of the orthologous proteins, like MPF2 and PFMAGO, might be maintained during evolution. As we showed here, *Arabidopsis* AGL24 and *Physalis* MPF2 share an overlapping set of interacting factors in plants. MAGO NASHI, that is, PFMAGO in *P. floridana*, has similar interacting partners in plants and animals. This latter observation might reflect common selection forces in plants and animals during evolution.

Supplementary Material

Supplementary tables 1–4 are available at *Molecular Biology and Evolution* online (http://www.mbe.oxfordjournals.org/).

Literature Cited

Acevedo FG, Gamboa A, Paéz-Valencia J, Jiménez-García LF, Izaguirre-Sierra M, Alvarez-Buylla ER. 2004. FLOR1, a putative interaction partner of the floral homeotic protein AGAMOUS, is a plant-specific intracellular LRR. Plant Sci. 167:225–231.

Ampomah-Dwamena C, Morris BA, Sutherland P, Veit B, Yao JL. 2002. Down-regulation of *TM29*, a tomato *SEPALLATA* homolog, causes parthenocarpic fruit development and floral reversion. Plant Physiol. 130(2):605–617.

Becker A, Theissen G. 2003. The major clades of MADS-box genes and their role in the development and evolution of flowering plants. Mol Phylogenet Evol. 29(3): 464–489.

Bono F, Ebert J, Unterholzner L, Guttler T, Izaurralde E, Conti E. 2004. Molecular insights into the interaction of PYM with the Mago-Y14 core of the exon junction complex. EMBO Rep. 5(3):304–310.

Boswell RE, Prout ME, Steichen JC. 1991. Mutations in a newly identified *Drosophila melanogaster* gene, *mago nashi*, disrupt germ cell formation and result in the formation of mirror-image symmetrical double abdomen embryos. Development. 113(1):373–384.

Causier B, Castillo R, Zhou J, Ingram R, Xue Y, Schwarz-Sommer Z, Davies B. 2005. Evolution in action: following function in duplicated floral homeotic genes. Curr Biol. 15(16):1508–1512.

Causier B, Cook H, Davies B. 2003. An Antirrhinum ternary complex factor specifically interacts with C-function and SEPALLATA-like MADS-box factors. Plant Mol Biol. 52:1051–1062.

Davies B, Egea-Cortines M, de Andrade Silva E, Saedler H, Sommer H. 1996. Multiple interactions amongst floral homeotic MADS box proteins. EMBO J. 15:4330–4343.

Davies B, Motte P, Keck E, Saedler H, Sommer H, Schwarz-Sommer Z. 1999. PLENA and FARINELLI: redundancy and regulatory interactions between two Antirrhinum MADS-box factors controlling flower development. EMBO J. 18:4023–4034.

de Folter S, Immink RGH, Kieffer M, et al. (12 co-authors) 2005. Comprehensive interaction map of the Arabidopsis MADS Box transcription factors. Plant Cell. 17(5):1424–1433.

Duttweiler HM. 1996. A highly sensitive and non-lethal ß-galactosidase plate assay for yeast. Trends Genet. 12: 340–341.

Egea-Cortines M, Saedler H, Sommer H. 1999. Ternary complex formation between the MADS-box proteins SQUAMOSA, DEFICIENS and GLOBOSA is involved in the control of floral architecture in *Antirrhinum majus*. EMBO J. 18:5370–5379.

Fribourg S, Gatfield D, Izaurralde E, Conti E. 2003. A novel mode of RBD-protein recognition in the Y14-Mago complex. Nat Struct Biol. 10(6):433–439.

Fujita H, Takemura M, Tani E, Nemoto K, Yokota A, Kohchi T. 2003. An Arabidopsis MADS-box protein, AGL24, is specifically bound to and phosphorylated by meristematic receptor-like kinase (MRLK). Plant Cell Physiol. 44:735–742.

Gamboa A, Paéz-Valencia J, Acevedo GF, Vázquez-Moreno L, Alvarez-Buylla RE. 2001. Floral transcription factor AGAMOUS interacts in vitro with a leucine-rich repeat and an acid phosphatase protein complex. Biochem Biophys Res Commun. 288:1018–1026.

Garcia-Maroto F, Ortega N, Lozano R, Carmona MJ. 2000. Characterization of the potato MADS-box gene *STMADS16* and expression analysis in tobacco transgenic plants. Plant Mol Biol. 42:499–513.

Hachet O, Ephrussi A. 2001. Drosophila Y14 shuttles to the posterior of the oocyte and is required for *oskar* mRNA transport. Curr Biol. 11(21):1666–1674.

Hachet O, Ephrussi A. 2004. Splicing of *oskar* RNA in the nucleus is coupled to its cytoplasmic localization. Nature. 428(6986):959–963.

He CY, Münster T, Saedler H. 2004. On the origin of floral morphological novelties. FEBS Lett. 567:147–151.

He CY, Saedler H. 2005. Heterotopic expression of *MPF2* is the key to the evolution of the Chinese lantern of Physalis, a morphological novelty in Solanaceae. Proc Natl Acad Sci USA. 102:5779–5784.

He CY, Saedler H. 2007. Hormonal control of the inflated calyx syndrome, a morphological novelty, in Physalis. Plant J. 49(5):935–946.

He CY, Zhang JS, Chen SY. 2002. A soybean gene encoding a proline-rich protein is regulated by salicylic acid, an endogenous circadian rhythm and by various stresses. Theor Appl Genet. 104:1125–1131.

Heyd F, ten Dam G, Möröy T. 2006. Auxiliary splice factor U2AF26 and transcription factor Gfi1 cooperate directly in

regulating CD45 alternative splicing. Nat Immunol. 7: 859–867.

Higo K, Ugawa Y, Iwamoto M, Korenaga T. 1999. Plant cis-acting regulatory DNA elements (PLACE) database. Nucleic Acids Res. 27:297–300.

Hileman LC, Sundstrom JF, Litt A, Chen M, Shumba T, Irish VF. 2006. Molecular and phylogenetic analyses of the MADS-box gene family in tomato. Mol Biol Evol. 23(11): 2245–2258.

Honma T, Goto K. 2001. Complexes of MADS-box proteins are sufficient to convert leaves into floral organs. Nature. 409: 525–529.

Johnson MA, von Besser K, Zhou Q, Smith E, Aux G, Patton D, Levin JZ, Preuss D. 2004. Arabidopsis *hapless* mutations define essential gametophytic functions. Genetics. 68(2): 971–982.

Karlova R, Boeren S, Russinova E, Aker J, Vervoort J, de Vries S. 2006. The *Arabidopsis* SOMATIC EMBRYOGENESIS RECEPTOR-LIKE KINASE1 protein complex includes BRASSINOSTEROID-INSENSITIVE1. Plant Cell. 18: 626–638.

Kataoka N, Diem MD, Kim VN, Yong J, Dreyfuss G. 2001. Magoh, a human homolog of Drosophila mago nashi protein, is a component of the splicing-dependent exon-exon junction complex. EMBO J. 20(22):6424–6433.

Kataoka N, Yong J, Kim VN, Velazquez F, Perkinson RA, Wang F, Dreyfuss G. 2000. Pre-mRNA splicing imprints mRNA in the nucleus with a novel RNA-binding protein that persists in the cytoplasm. Mol Cell. 6(3):673–682.

Kawano T, Kataoka N, Dreyfuss G, Sakamoto H. 2004. Ce-Y14 and MAG-1, components of the exon-exon junction complex, are required for embryogenesis and germline sexual switching in *Caenorhabditis elegans*. Mech Dev. 121(1):27–35.

Kim VN, Yong J, Kataoka N, Abel L, Diem MD, Dreyfuss G. 2001. The Y14 protein communicates to the cytoplasm the position of exon-exon junctions. EMBO J. 20(8):2062–2068.

Lau CK, Diem MD, Dreyfuss G, Van Duyne GD. 2003. Structure of the Y14-Magoh core of the exon junction complex. Curr Biol. 13(11):933–941.

Le Hir H, Gatfield D, Braun IC, Forler D, Izaurralde E. 2001. The protein Mago provides a link between splicing and mRNA localization. EMBO Rep. 2(12):1119–1124.

Li W, Boswell R, Wood WB. 2000. *mag-1*, a homolog of Drosophila *mago nashi*, regulates hermaphrodite germ-line sex determination in *Caenorhabditis elegans*. Dev Biol. 218(2):172–182.

Ling M, Merante F, Robison BR. 1995. A rapid and reliable DNA preparation method for screening a large number of yeast clones by polymerase chain reaction. Nucleic Acids Res. 23:4924–4925.

Mandel MA, Gustafson-Brown C, Savidge B, Yanofsky MF. 1992. Molecular characterization of the Arabidopsis floral homeotic gene *APETALA1*. Nature. 360:273–277.

Masiero S, Imbriano C, Ravasio F, Favaro R, Pelucchi N, Gorla MS, Mantovani R, Colombo L, Kater MM. 2002. Ternary complex formation between MADS-box transcription factors and the histone fold protein NF-YB. J Biol Chem. 277:26429–26435.

Masiero S, Li MA, Will I, Hartmann U, Saedler H, Huijser P, Schwarz-Sommer Z, Sommer H. 2004. *INCOMPOSITA*: a MADS-box gene controlling prophyll development and floral meristem identity in Antirrhinum. Development. 131(23):5981–5990.

Micklem DR, Dasgupta R, Elliott H, Gergely F, Davidson C, Brand A, Gonzalez-Reyes A, St Johnston D. 1997. The *mago nashi* gene is required for the polarisation of the oocyte and the formation of perpendicular axes in Drosophila. Curr Biol. 7(7):468–478.

Mohr SE, Dillon ST, Boswell RE. 2001. The RNA-binding protein Tsunagi interacts with Mago Nashi to establish polarity and localize *oskar* mRNA during Drosophila oogenesis. Genes Dev. 15(21):2886–2899.

Newmark PA, Boswell RE. 1994. The *mago nashi* locus encodes an essential product required for germ plasm assembly in Drosophila. Development. 120(5):1303–1313.

Newmark PA, Mohr SE, Gong L, Boswell RE. 1997. mago nashi mediates the posterior follicle cell-to-oocyte signal to organize axis formation in Drosophila. Development. 124(16):3197–3207.

Pagnussat GC, Yu HJ, Ngo QA, Rajani S, Mayalagu S, Johnson CS, Capron A, Xie LF, Ye D, Sundaresan V. 2005. Genetic and molecular identification of genes required for female gametophyte development and function in *Arabidopsis*. Development. 132(3):603–614.

Pelaz S, Gustafson-Brown C, Kohalmi SE, Crosby WL, Yanofsky MF. 2001. APETALA1 and SEPALLATA3 interact to promote flower development. Plant J. 26:385–394.

Roth FP, Hughes JD, Estep PW, Church GM. 1998. Finding DNA regulatory motifs within unaligned noncoding sequences clustered by whole-genome mRNA quantitation. Nat Biotechnol. 16(10):939–945.

Schwarz-Sommer Z, Hue I, Huijser P, Flor PJ, Hansen R, Tetens F, Lönnig W-E, Saedler H, Sommer H. 1992. Characterization of the Antirrhinum floral homeotic MADS-box gene *deficiens*: evidence for DNA binding and autoregulation of its persistent expression throughout flower development. EMBO J. 11:251–263.

Shi H, Xu RM. 2003. Crystal structure of the Drosophila Mago nashi-Y14 complex. Genes Dev. 17(8):971–976.

Sommer H, Beltran J-P, Huijser P, Pape H, Lonnig W-E, Saedler H, Schwarz-Sommer Z. 1990. *Deficiens*, a homeotic gene involved in the control of flower morphogenesis in *Antirrhinum majus*: the protein shows homology to transcription factors. EMBO J. 9:605–613.

Stroupe ME, Tange TO, Thomas DR, Moore MJ, Grigorieff N. 2006. The three-dimensional architecture of the EJC core. J Mol Biol. 360(4):743–749.

Swidzinski JA, Zaplachinski ST, Chuong SD, Wong JF, Muench DG. 2001. Molecular characterization and expression analysis of highly conserved rice *mago nashi1* homolog. Genome. 44:394–400.

Takemura M, Sawai R, Kohchi T. 2004. Proceedings of the 15th International Conference on Arabidopsis Research; 2004 July 11-14; Berlin, Germany. Abstract T01-014, p. 93; www.arabidopsis.org/news/15ArabAbstract.pdf.

Tange TO, Shibuya T, Jurica MS, Moore MJ. 2005. Biochemical analysis of the EJC reveals two new factors and a stable tetrameric protein core. RNA. 11(12):1869–1883.

Theissen G. 2001. Development of floral organ identity: stories from the MADS house. Curr Opin Plant Biol. 4:75–85.

Theissen G, Saedler H. 2001. Plant biology: floral quartets. Nature. 409:469–471.

Thijs G, Lescot M, Marchal K, Rombauts S, De Moor B, Rouzé P, Moreau Y. 2001. A higher order background model improves the detection of regulatory elements by Gibbs sampling. Bioinformatics. 17(12):1113–1122.

Tröbner W, Ramirez L, Motte P, Hue I, Huijser P, Lönnig W-E, Saedler H, Sommer H, Schwarz-Sommer Z. 1992. GLOBOSA: a homeotic gene which interacts with DEFICIENS in the control of Antirrhinum floral organogenesis. EMBO J. 11(13):4693–4704.

Tzeng T-Y, Liu H-C, Yang C-H. 2004. The C-terminal sequence of LMADS1 is essential for the formation of homodimers for B function proteins. J Biol Chem. 279(11):10747–10755.

Yanofsky MF, Ma H, Bowman JL, Drews GN, Feldmann KA, Meyerowitz EM. 1990. The protein encoded by the Arabidopsis homeotic gene *AGAMOUS* resembles transcription factors. Nature. 346:35–39.

Yu H, Ito T, Wellmer F, Meyerowitz EM. 2004. Repression of *AGAMOUS-LIKE 24* is a crucial step in promoting flower development. Nat Genet. 36:157–161.

Zhao XF, Colaizzo-Anas T, Nowak NJ, Shows TB, Elliott RW, Aplan PD. 1998. The mammalian homologue of *mago nashi* encodes a serum-inducible protein. Genomics. 47(2):319–322.

Zhao XF, Nowak NJ, Shows TB, Aplan PD. 2000. MAGOH interacts with a novel RNA-binding protein. Genomics. 63(1):145–148.

Zimmermann P, Hirsch-Hoffmann M, Hennig L, Gruissem W. 2004. GENEVESTIGATOR. Arabidopsis microarray database and analysis toolbox. Plant Physiol. 136:2621–2632.

William Martin, Associate Editor

Accepted February 27, 2007